Soft Matter

Cite this: *Soft Matter*, 2011, **7**, 3011

www.rsc.org/softmatter

PAPER

In situ synthesized Ag nanoparticle in self-assemblies of amino acid based amphiphilic hydrogelators: development of antibacterial soft nanocomposites†

Anshupriya Shome, Sounak Dutta, Subhabrata Maiti and Prasanta Kumar Das*

Received 1st October 2010, Accepted 4th January 2011
DOI: 10.1039/c0sm01087a

The present work reports the development of a new class of antibacterial soft-nanocomposites by *in situ* synthesis of silver nanoparticle (AgNP) within the supramolecular self-assemblies of amino acid (tryptophan/tyrosine) based amphiphilic hydrogelators. Interestingly, the nanoparticle synthesis does not require the use of any external reducing/stabilizing agents. The nanocomposites were characterized by UV-vis spectra, transmission electron microscopy (TEM) images, X-ray diffraction spectroscopy (XRD) and thermo gravimetric analysis (TGA). Encouragingly, these soft nanocomposites showed excellent antibacterial activity against both Gram-positive and Gram-negative bacteria whereas the amphiphiles alone were lethal only toward Gram-positive bacteria. Judicious combination of bactericidal AgNP within the self-assemblies of inherently antibacterial amphiphilic gelators led to the development of soft nanocomposites effective against both type of bacteria. The head group charge and structure of the amphiphiles were altered to investigate their important role on the synthesis and stabilization of AgNP and also in modulating the antibacterial activity of the nanocomposites. The antibacterial activities of soft nanocomposites comprising amphiphiles with cationic head group were found to be more efficient than the anionic soft nanocomposites. Interestingly, these nanocomposites have shown considerable biocompatibility to mammalian cell, NIH3T3. Furthermore, the well-known tissue engineering scaffold, agar-gelatin film infused with these soft nanocomposites allowed normal growth of mammalian cells on its surface while being lethal toward both Gram-positive and Gram-negative bacteria.

Introduction

Design and development of new antibacterial agents is finding unremitting significance, particularly in bio-medicinal chemistry, due to the growing resistance of bacteria against conventional antibiotics.[1–3] To combat this ever increasing threat from pathogens, the inventory of existing antibiotics needs to be constantly upgraded with materials having newer modes of killing. In this context, silver nanoparticles (AgNPs) are emerging as efficient antimicrobial agents because of their difference in the mechanism of killing bacteria.[4–7] Importantly, in contrast to the common antibiotics, to date no bacterial resistance against AgNPs has been reported.[4,6,7] However, the AgNPs are known to exhibit superior antibacterial activity against Gram-negative bacteria compared to that of Gram-positive bacteria.[8,9] Therefore AgNP based hybrid systems comprising a complementary antibacterial agent with proven efficacy against Gram-positive bacteria can lead to the development of versatile antibacterial nanocomposites. Again, it would be indeed beneficial if that antibacterial agent in the composite can simultaneously reduce the silver ion and stabilize the AgNP instead of using external reducing agents. Also, the reducing and stabilizing agents should be preferably biocompatible for the proper utilization of AgNP-composites in biomedicine including tissue engineering, drug delivery and so forth.[4a,10,11] In this regard, the presence of natural precursors like amino acid, sugar moiety and so forth in the structure of reducing/stabilizing agent is expected to introduce biocompatibility within the nanocomposite.[4a,7,10–12]

To this end, we have recently shown the efficient killing of Gram-positive bacteria by aromatic amino acid-based amphiphilic hydrogelators.[13,14] The mode of bacteria killing by these positively charged gelators includes the disruption of cell membrane, which results in the release of cytoplasmic constituents leading to cell death.[1,13,14] However, these amphiphilic

Department of Biological Chemistry, Indian Association for the Cultivation of Science, Jadavpur, Kolkata, 700 032, India. E-mail: bcpkd@iacs.res.in; Fax: +(91)-33-24732805

† Electronic supplementary information (ESI) available: Zone of Inhibition for agar-gelatin films containing soft nanocomposites, TEM images of lyophilized nanocomposites, the fluorescence micrograph of *E. coli* and *S. aureus* before and after treating with AgNP-**1** composites in presence of LIVE/DEAD® BacLight™ Bacterial Viability Kit, antibacterial activity of agar-gelatin films against *B. Subtilis*, fluorescence images of NIH3T3 cells incubated on agar-gelatin films containing AgNP-**3** and AgNP-**4** composites stained with LIVE/DEAD® Viability/Cytotoxicity Kit for mammalian cells. See DOI: 10.1039/c0sm01087a

gelators with C-16 chain length were unable to kill Gram-negative bacteria even at high concentrations presumably due to the existence of an outer layer consisting of lipopolysaccharide and phospholipids in addition to the peptidoglycan layer as present in Gram-positive bacteria.[13–16] Thus, it is important to develop systems, which will be equally efficient against both Gram-positive and Gram-negative bacteria. In this context, previously[13] we have reduced the alkyl chain length to make the amphiphile (**1**) effective against both types of bacteria. But cytotoxicity of amphiphile was found to be increased with decrease in chain length. This higher toxicity of nano-composites synthesized from short chain amphiphiles will of course reduce the scope of their biomedicinal applications. So inclusion of AgNP within the self-assembled network of these biocompatible cationic C-16 hydrogelators would be very intriguing with respect to the killing of Gram-negative bacteria by AgNPs. As the amphiphiles are intrinsically bactericidal against Gram-positive bacteria, it is expected that the AgNP based soft nanocomposites will have killing effects against both types of bacteria. Considering the biocompatibility of these soft nanocomposites it is preferable to synthesize AgNP *in situ* within the self-assemblies of non-toxic hydrogelating amphiphiles.

In the present work, novel soft nanocomposites have been developed by the *in situ* synthesis of AgNP in the supramolecular self-assemblies of aromatic amino acid (tryptophan and tyrosine) based amphiphilic hydrogelators with varying head group structure (**1–4**, Chart 1). The formation of these soft nanocomposites was characterized by spectroscopic and microscopic techniques. Encouragingly, the nanocomposites have shown excellent antibacterial activity against both Gram-positive and Gram-negative bacteria with minimum inhibitory concentration (MIC), 10–50 μg mL^{-1} whereas the amphiphiles alone were either lethal toward only Gram-positive bacteria or ineffective against any type of bacteria. Moreover, as confirmed by MTT (3-(4,5-dimethyl-2-thiazolyl)-2,5-diphenyl-2*H*-tetrazolium bromide) assay, these self-assembled AgNP-composites were found to be biocompatible to mammalian cells, NIH3T3. Interestingly, the well-known tissue engineering scaffold,[17] agar-gelatin film infused with these soft nanocomposites allowed normal growth of mammalian cells on its surface while being lethal toward bacteria.

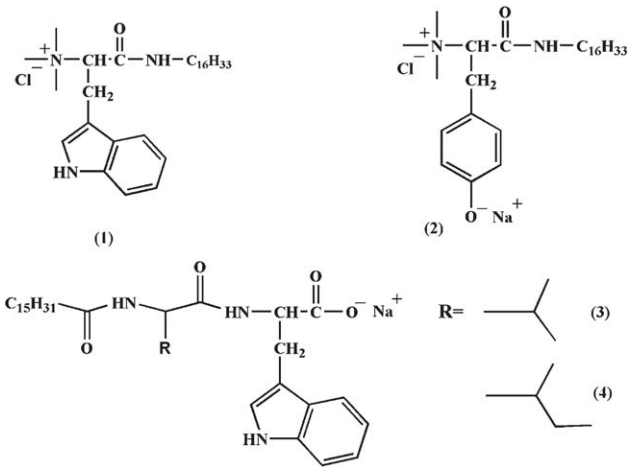

Chart 1 Structure of amphiphilic hydrogelators.

Results and discussion

Development of new antibacterial materials by the judicious combination of AgNPs with soft materials like hydrogels would be of great significance as the resultant soft nanocomposites will find huge applications in biomedicine.[18] In the present work, AgNP based soft nanocomposites were developed by *in situ* synthesis of AgNP within the supramolecular self-assemblies of aromatic amino acid based amphiphilic hydrogelators (**1–4**, Chart 1). The head group structure and charge of the amphiphiles were varied to find their effect on the *in situ* synthesis of AgNPs and also on the antibacterial activity of nanocomposites. The polar head of amphiphiles are comprised of aromatic amino acids, L-tryptophan for **1**, **3** and **4** and L-tyrosine in case of **2**. These two redox active amino acids are well known for reducing silver and gold ions to corresponding nanoparticles.[19–22] Also the presence of naturally occurring amino acids in these amphiphiles is advantageous for biocompatibility of the soft composites.[13,14] All these amphiphiles have excellent water gelation ability as large volume of water gets entrapped within the supramolecular self-assemblies of these gelators.[23,24] Among them, amphiphile **1** forms most efficient hydrogel with a minimum gelation concentration (MGC) of 0.3%, w/v (6 mM). Physical gelation is the manifestation of self-assemblies of amphiphiles at MGC; however the process of self-assembly starts at much lower concentration of gelator than MGC.[24] With increasing concentration of amphiphile, the supramolecular self-assembly leads to the formation of hydrogel. This self-assembled network of the redox active amino acid based gelators is utilized for *in situ* synthesis of AgNPs.

Synthesis of AgNP within the self-assemblies of amphiphilic hydrogelators

The critical concentrations at which the amphiphiles, **1–4** begin to self-assemble in water (critical micellar concentration) are 0.13, 0.08, 0.04 and 0.06 mM, respectively.[25] To ensure the synthesis and stabilization of AgNP within the self-assemblies of the hydrogelator, the concentration of amphiphiles was always kept higher than the said critical concentrations. Tollens' reagent was used for the synthesis of AgNP within the self-assemblies of all the amphiphiles. To achieve the optimum reaction condition for *in situ* synthesis of AgNP, concentration ratio of hydrogelators to Tollens' reagent was varied from 1 : 1 to 10 : 1 and also the temperature of reaction mixtures changed from 60 to 120 °C. The said parameters needed for the efficient *in situ* synthesis of AgNP were found to be dependent on the structure and self-assembling behaviour of amphiphiles. In case of **1**, Tollens' reagent was added to the hot (80 °C) aqueous solution of amphiphile (0.2 mM) with 1 : 1 concentration ratio and the mixture was stirred at 80 °C. Initially, the AgNP formation was indicated by the change of the visual appearance of solution from colourless to yellow. The formation of AgNP was followed by monitoring surface plasmon resonance (SPR) peak of the nanoparticle at 413 nm in time dependent UV-visible spectra (Fig. 1A). At the said concentrations of amphiphile **1** and silver ion, it took almost 4 h to complete the synthesis of AgNP (Fig. 1A). However, in case of other three hydrogelators (**2–4**), the required concentration ratio between amphiphiles and Tollens' reagent was 10 : 1 (2 mM: 0.2 mM) and the needed reaction temperatures were 70, 100 and 120 °C,

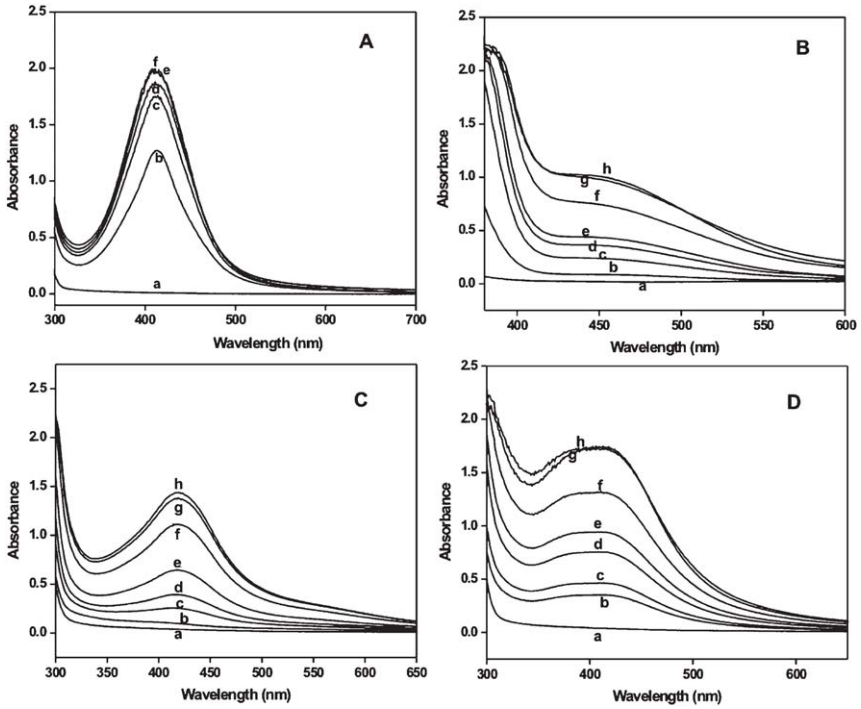

Fig. 1 Time dependent UV-vis spectra of *in situ* synthesized AgNPs by amphiphile **1** (A) at a: 0; b: 1; c: 2; d: 3; e: 4; f: 5 h, **2** (B) at a: 0; b: 1; c: 2; d: 3; e: 4; f: 5; g: 6 h: 7 h **3** (C) and **4** (D) a: 0; b: 5; c: 8; d: 12; e: 24; f: 36; g: 48; h: 56 h.

respectively. The characteristic SPR peaks of AgNP were observed at 410–450 nm depending on the amphiphiles (Fig. 1B–D). In case of tyrosinate amphiphile (**2**), *in situ* reduction of silver ion was completed within 6 h whereas that took much longer time (~2 days) for two negatively charged tryptophan based dipeptide amphiphiles (**3** and **4**). Interestingly, the concentration of **1** required (0.2 mM) for the synthesis of AgNPs is 10 times lower compared to that which was used for the other three amphiphiles (**2–4**). Both tryptophan and tyrosinate moieties present at the headgroup of amphiphiles **1** and **2**, respectively are very efficient in synthesizing AgNPs by reducing the silver ion. The high concentration of **2** (2 mM) was needed for the synthesis of AgNP possibly due to the weaker self-assembled networking of **2** in comparison to that of **1**. This difference in the supramolecular organization led to the formation of weak hydrogel for amphiphile **2** with a MGC of ~4%, w/v (82 mM), which is ~14 times higher than that of amphiphile **1** (0.3%, w/v; 6 mM).[23] Even in case of **3** and **4**, despite having the same redox active amino acid tryptophan in the polar head as in **1**, high amphiphile concentration (2 mM) as well as more rigorous conditions (high temperature and long time) was needed for the synthesis of Ag nanocomposites. Here also the self-assembling ability is not very efficient as almost 5 times higher MGC, 30 and 29 mM, respectively were observed for **3** and **4** compared to that of **1**.[23] Thus, the self-assembled network of amphiphiles have a crucial influence in the synthesis of soft nanocomposite particularly in terms of stabilizing the nanoparticle. The self-assembling properties of these amphiphiles coupled with their *in situ* metal ion reducing ability facilitate the development of AgNP based soft nanocomposites. The synthesized AgNP was centrifuged at 30,000 rpm and washed thrice with Milli-Q water to remove the excess silver ions. The pellet was dispersed in 0.2 mM surfactant solution (5 mL) and lyophilized to obtain nanocomposite powder. This powder was then weighed and re-dispersed in known volume of water to prepare desired concentration of nanocomposites for antibacterial and biocompatibility studies.

Transmission electron microscopy (TEM) images

The AgNP formation within the self-assemblies of amphiphiles was characterized by acquiring the TEM images of soft nanocomposites before centrifugation (Fig. 2a–d). The AgNPs were found to be spherical in nature irrespective of the amphiphile used. The sizes of the nanoparticles were in the range of 10–25 nm (Fig. 2). The formation of AgNPs within the self-assemblies of amphiphiles was also evident from the observed supramolecular networks in the respective TEM images of AgNP-**1** to **4**. At this point, it was also important to know whether the shape and the size of AgNPs were retained after centrifugation/lyophilization since the re-dispersed lyophilized powders of AgNP-composites in water were used for antibacterial activity and biocompatibility studies. Therefore, the aqueous solution of lyophilized AgNP-composite was also characterized by TEM images (Fig. S1, see ESI†). Interestingly, the spherical nanoparticles with 10–25 nm size were found to be encapsulated within the supramolecular network of amphiphiles as observed before centrifugation (Fig. 2). Supramolecular networks of the amphiphiles in absence of nanoparticles were also evident from their TEM images (Fig. S2, ESI†).

X-ray diffraction (XRD)

Formation of AgNPs was further confirmed by XRD experiments. XRD spectra of the soft nanocomposites revealed distinct

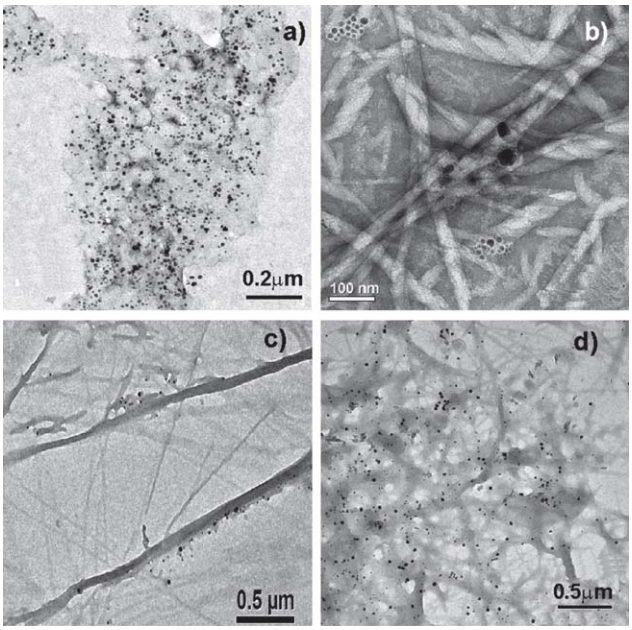

Fig. 2 TEM images of AgNP synthesized within self-assemblies of amphiphiles **1** (a), **2** (b),**3** (c) and **4** (d).

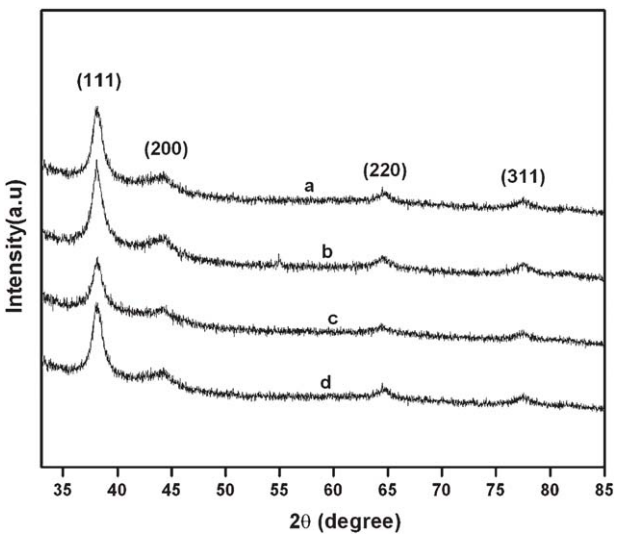

Fig. 3 XRD patterns of the AgNP based nanocomposites of hydrogelator **1** (a), **2** (b), **3** (c) and **4** (d).

four peaks (Fig. 3), which are characteristics for Ag nanocrystal. The observed peaks at 38.09° (111), 44.28° (200), 64.54° (220), and 77.42° (311) were in agreement with the respective planes of crystalline Ag nanoparticles (Fig. 3).[26]

Quantification of amphiphiles and AgNP in the nanocomposites

The amount of amphiphile present in the nanocomposites was measured by UV-vis spectroscopy and thermogravimetric analysis (TGA). All the hydrogelators (**1–4**) showed a strong absorption band at 270–280 nm due to π–π* transition of aromatic moieties present in the amphiphiles. A standard calibration curve was prepared by measuring the absorbance at varying concentration of amphiphiles. The amount of amphiphile present in the nanocomposite was determined from the calibration curve of amphiphile. Finally, the amount of AgNP in the nanocomposite was observed to be 28 to 56% (Table 1) depending on the amphiphiles. AgNP content in the nanocomposites was also determined by TGA.[27] In contrast to the pure amphiphile **1**, which left negligible residue after 400 °C (Fig. 4a), the AgNP-**1** composite showed the presence of considerable amount of residue of AgNP after sharp weight loss between 200 and 400 °C (Fig. 4b). Almost 60% weight was lost between 200 and 400 °C that correspond to the decomposition of amphiphile. Thus, the weight percent of AgNP in AgNP-**1** composite was 40%, which is in good agreement with the estimated AgNP content from UV-vis absorption spectroscopy (Table 1).

Table 1 % of AgNP in the soft nanocomposites

AgNP based nanocomposites	% of AgNP
1	37
2	28
3	56
4	37

Antibacterial activity

The antibacterial activity of the amphiphilic hydrogelators as well as the AgNP based nanocomposites of **1–4** was investigated using two Gram-positive bacteria *Bacillus subtilis* (*B. subtilis*), *Staphylococcus aureus* (*S. aureus*) and three Gram-negative bacteria *Escherichia coli* (*E. coli*), *Klebsiella aerogenes* (*K. aerogenes*) and *Klebsiella pneumoniae* (*K. pneumoniae*). Antibacterial activity was checked in nutrient agar media by spread plate method.

The amphiphiles (**1–2**) with quaternary ammonium head group were highly effective against Gram-positive bacteria *B. subtilis* and *S. aureus* having MIC of 1–10 μg mL^{-1} (Table 2). The killing of Gram-positive bacteria by the amphiphile **1** is consistent with the previous reports.[13] On the contrary, the amphiphiles with negatively charged head group (**3–4**) were

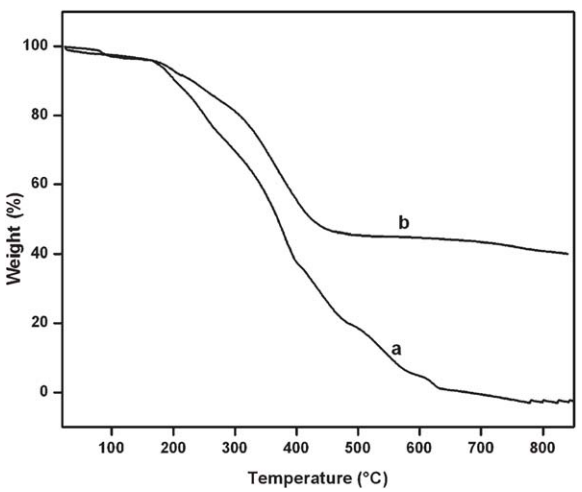

Fig. 4 TGA thermograms of **1** (a) and AgNP-**1** composite (b).

Table 2 MIC of amphiphiles and soft nanocomposites[a] in μg mL^{-1}

	B. subtilis (gm +ve)	*S. aureus* (gm +ve)	*E. coli* (gm −ve)	*K. aerogenes* (gm −ve)	*K. pneumoniae* (gm −ve)
1	10	1	—	—	—
AgNP-**1**	20 (7.4)	10 (3.7)	60 (22.2)	80 (29.6)	50 (18.5)
2	10	5	—	—	—
AgNP-**2**	20 (7.8)	10 (2.8)	75 (21)	55 (15.4)	60(16.8)
3	200	—	—	—	—
AgNP-**3**	100 (56)	150 (84)	150 (84)	75 (42)	75 (42)
4	—	—	—	—	—
AgNP-**4**	200 (74)	200 (74)	200 (74)	100 (37)	150 (55.5)

[a] Value given in the parentheses describes the AgNP content in the composites.

unable to show antibacterial activity against these two bacteria except in the case of **3** that killed *B. subtilis* at a very high MIC, 200 μg mL^{-1}. The outer wall of Gram-positive bacteria is composed of peptidoglycan layer, which is negatively charged due to the presence of phosphoryl groups located in the substituent teichoic and techuronic acid residues as well as carboxylate groups.[28] The cationic charge of the amphiphiles **1** and **2** helped them to interact with the negatively charged cell membrane of the bacteria. This electrostatic interaction is also entropically favoured as a large number of counter ions from the cell membrane are released.[29] The lipophilic residues of the amphiphiles then undergo 'self-promoted' transport across the bacterial membrane followed by the disruption of the cell membrane and release of cytoplasmic constituents leading to death of bacteria.[30–33] However, this process of bacteria killing could not take place for anionic amphiphiles (**3–4**) possibly because of no favourable interaction with negatively charged cell membrane of bacteria. In case of Gram-negative bacteria, none of the hydrogelators (**1–4**) exhibited any antibacterial activity even up to the concentration of 200 μg mL^{-1} (Table 2). In case of Gram-negative bacteria the peptidoglycan layer is shielded by an additional outer membrane consisting of lipopolysaccharide and phospholipids and thus is not exposed to the extracellular environment.[28] So the cationic amphiphiles (**1–2**) cannot interact with the outer cell-membrane as efficiently as in case of Gram-positive bacteria.

Importantly, the soft nanocomposites of AgNP showed broad-spectrum antibacterial activity against both Gram-positive and Gram-negative bacteria (Table 2). For Gram-positive bacteria, the MIC of AgNP-**1** and AgNP-**2** was found to be 10–20 μg mL^{-1} against *B. subtilis* and *S. aureus*. Incorporation of AgNP additionally could not improve the antibacterial activity of the composites possibly because of the very efficient inherent killing ability (MIC-1-10 μg mL^{-1}) of the amphiphiles (**1** and **2**). The effect of AgNP was rather observed for AgNP-**3** and AgNP-**4** composites. These nanocomposites were able to kill Gram-positive bacteria, although at reasonably high MIC (100–200 μg mL^{-1}) where the contribution of AgNP was in the range of 56–84 μg mL^{-1} (Table 2). Notably, the AgNP induces the antibacterial activity within the soft nanocomposites of negatively charged amphiphilic hydrogelators, **3** and **4**. Encouragingly, in contrast to the individual amphiphiles, more efficient antibacterial activity of AgNP-composites was observed for Gram-negative bacteria. The MIC values of AgNP-**1** composite were 50–80 μg mL^{-1} (Table 2) with 18.5–29.6 μg mL^{-1} AgNP content (determined using Table 1). AgNP-**2** also showed similar killing efficiency against Gram-negative bacteria having MIC value of 55–75 μg mL^{-1} (15.4–21 μg mL^{-1} AgNP). However, the MIC values for AgNP-**3** (75–150 μg mL^{-1} containing 42–84 μg mL^{-1} AgNP) and AgNP-**4** (100–200 μg mL^{-1} having 37–74 μg mL^{-1} AgNP) against Gram-negative bacteria were comparatively higher than that of AgNP-**1/2** composites. The variation in the antibacterial efficiency of different nanocomposites is presumably due to the effect of amphiphile's head group structure, size as well as its charge density. Most importantly, while the individual amphiphiles were completely incapable of killing Gram-negative bacteria, the AgNP-based soft nanocomposites of same amphiphiles were lethal to both Gram-positive and Gram-negative bacteria.

This wide spectrum antibacterial activity of the soft nanocomposites is primarily because of the intrinsic bactericidal efficiency of AgNP through multimodal mechanism in conjugation with the killing efficacy of amphiphiles. Although the reason behind the antibacterial activity of AgNP is not entirely understood, the possible mechanisms of action were proposed in various reports.[4,11,34] The AgNP can get attached to the cell surface of bacteria as well as interact with the sulphur containing protein present in cell membrane, which will hinder the normal cellular functions leading to the cell death. AgNP can also penetrate inside the bacterial cell where it can interact with phosphorus containing DNA or attack the mitochondria resulting in permanent damage to bacteria. In addition, the AgNP can release silver ion inside the bacterial cell resulting oxidative stress responsible for antibacterial activity. As a whole, the soft composite of AgNP with quaternary ammonium moiety integrated in head group of the amphiphile (AgNP-**1/2**) showed better antibacterial efficacy than the soft nanocomposites of negatively charged amphiphiles, **3/4**. It is clear from the antibacterial activity of AgNP-**3/4**, AgNP in these nanocomposites showed its antibacterial activity in different mechanisms other than only electrostatic interactions. As mentioned above, the cationic charge around the nanoparticles in AgNP-**1/2** can easily localized the bactericidal AgNP to the negatively charged cell membrane of bacteria resulting in better antibacterial efficiency compared to AgNP-**3/4**. Although **2** contains an extra negative charge in its polar head, the presence of quaternary ammonium group helped it to exhibit higher antibacterial efficiency like AgNP-**1**. Hence, the multimodal bactericidal efficiency of AgNP in combination with the inherent bacterial killing ability of amphiphiles made these soft nanocomposites effective against both Gram-positive and Gram-negative bacteria.

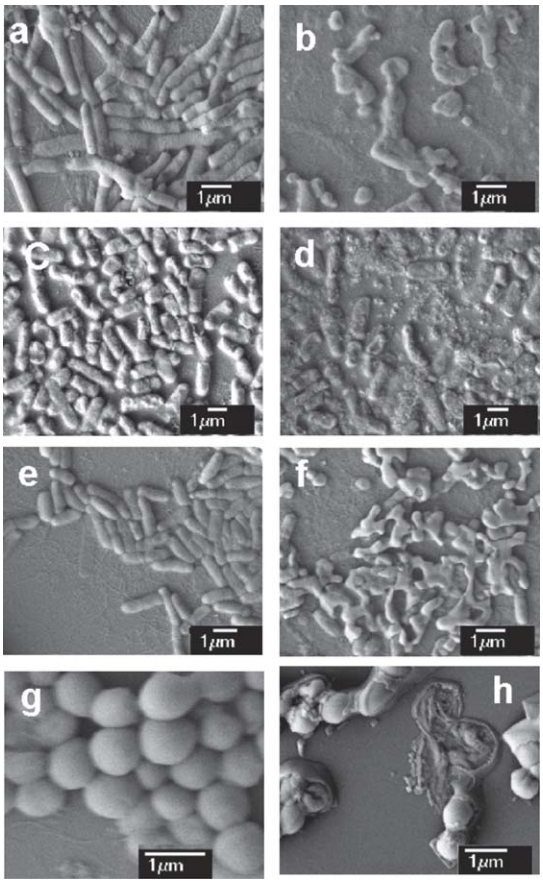

Fig. 5 SEM images of bacteria *E. coli* (a-control, b-treated with 90 μg mL^{-1} AgNP-1) *K. aerogenes* (c-control, d-treated with 90 μg mL^{-1} AgNP-1) *B. subtilis* (e-control, f-treated with 25 μg mL^{-1} AgNP-1) and *S. Aureus* (g-control, h-treated with 25 μg mL^{-1} AgNP-1).

Scanning electron microscopy (SEM) images of bacteria

To get an insight into the effect of AgNP-composites on bacteria, the morphology of Gram-negative (*E. coli* and *K. aerogenes*) and Gram-positive bacteria (*B. subtilis* and *S. aureus*) were examined by taking their SEM images (Fig. 5)[35,36] before and after treatment with AgNP-**1** composite above MIC (90 μg mL^{-1} and 25 μg mL^{-1} for Gram-negative and Gram-positive bacteria). The incubation of bacteria with AgNP-**1** for 3–4 h showed a significant change in their cell morphology. The untreated bacteria *E. coli* (Fig. 5a), *K. aerogenes* (Fig. 5c), *B. subtilis* (Fig. 5e), and *S. aureus* (Fig. 5g) exhibited healthy cell morphology with preserved integrity of membrane structure. However, after treatment with the AgNP-**1** composite, the SEM images showed deformation in the structure of bacteria with compromised membrane integrity of *E. coli* (Fig. 5b), *K. aerogenes* (Fig. 5d), *B. subtilis* (Fig. 5f), and *S. aureus* (Fig. 5h).

Fluorescence microscopic imaging of bacteria

We have also studied the antibacterial activity of the AgNP-**1** composite by fluorescence microscopy using commercially available LIVE/DEAD® BacLight™ bacterial viability kit.[13,14,37] The kit contains two nucleic acid binding stains, SYTO 9 and propidium iodide. These dyes have different cell penetration properties along with distinct spectral characteristics. SYTO 9 binds to the nucleic acid of both living and dead cells and exhibits green fluorescence after excitation with BP460–495 nm filter. Propidium iodide only binds to the nucleic acid of dead cells and shows red fluorescence. The fluorescence microscopic images of untreated Gram-negative, *E. coli* and Gram-positive, *S. aureus* as well as that of same bacterial cells treated with 90 and 25 μg mL^{-1} of AgNP-**1** composite, respectively were shown in Fig. S3a and S3c (ESI†). All the untreated cells exhibited green fluorescence indicating the living status of bacteria. However, the observed red fluorescence in the microscopic images (Fig. S3b and S3d, ESI†) of AgNP-**1** treated bacteria further confirms the bactericidal efficiency of the nanocomposite.

Biocompatibility study

These newly developed antibacterial soft nanocomposites will find significance in biomedicinal applications only if they exhibit compatibility with eukaryotic cells. To this end, we investigated the cytotoxicity of the self-assembled nanocomposites to mammalian cells, NIH3T3. MTT based cell viability assay was used to test the cytotoxicity of nanocomposites in the concentration range of 10–200 μg mL^{-1}. AgNP based soft composites exhibited remarkable biocompatibility, as 85–90% cells remained alive up to 25 μg mL^{-1} of nanocomposite (Fig. 6). Even 65–80% mammalian cells were found to be viable at 75 μg mL^{-1} of composite. Interestingly, in this range of nanocomposite concentration, both Gram-positive and Gram-negative bacteria were killed by AgNP-**1** and AgNP-**2**. The nanocomposites also showed 45–60% viability of mammalian cells (Fig. 6) at 75–200 μg mL^{-1} where AgNP-**3** and AgNP-**4** are effective in killing both type of bacterial cell. The nanocomposites with negatively charged amphiphiles **3** and **4** have shown better cell viability than positively charged AgNP-**1** and AgNP-**2**. The quaternary ammonium group in **1** and **2** possibly has preference over the negatively charged amphiphiles to interact with the cell membrane of mammalian cells comprised with zwitterionic lipids. Most importantly, all the soft nanocomposites selectively attack the bacterial pathogens while they remain biocompatible

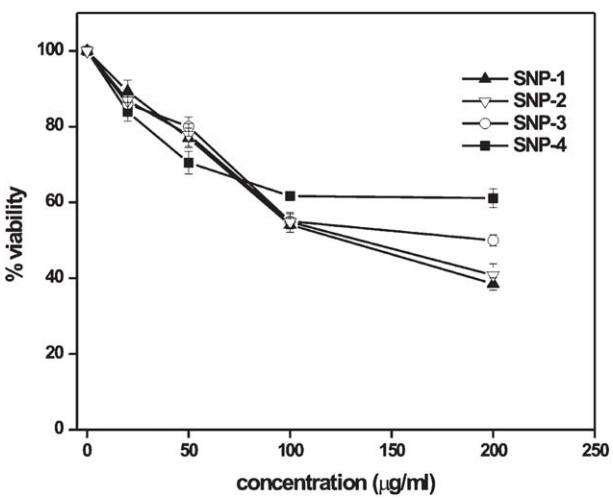

Fig. 6 MTT assay based percent cell viability as a function of concentration of AgNP based nanocomposites of amphiphile **1**–**4**.

to the mammalian cells. Such cell selectivity may have originated from the difference in the lipid composition of prokaryotic and eukaryotic cell membrane. The bacterial membranes are rich in negatively charged lipids for example phosphatidylglycerol and lipopolysaccharide, while the eukaryotic cell membranes are mainly composed of zwitterionic lipids such as phosphatidylcholine and sphingomyelin.[38] As a result, positively charged nanocomposites are more efficient in discriminating two types of the cells and preferentially bind to the more negatively charged bacterial membrane. Also, the thiol (–SH) containing protein present at the extra cellular membrane of bacteria facilitates its interaction with AgNP of soft nanocomposites due to the affinity of silver toward sulphur.[11]

Development of antibacterial and biocompatible film

The necessity of developing antibacterial materials for biomedicinal applications including tissue engineering is on the rise considering the material induced nosocomial infections in living systems.[39] To this end, utilization of these antibacterial soft nanocomposites in the development of functional biomaterials without compromising the biocompatibility would be of great importance. In this regard, Verma *et al.* recently reported the biocompatibility and growth of mice fibroblast cells (NIH3T3) on the surface of agar-gelatin (2 : 1) hydrogel cross-linked with glutaraldehyde.[17] Although these matrices are safe to eukaryotic cells but they don't have any inherent antimicrobial property. In order to bring in the antibacterial property within this matrix, we have infused the AgNP based soft nanocomposites into this agar-gelatin film and tested the antibacterial activity of these hybrid films. As expected, normal growth of *E. coli* and *B. subtilis* were seen in the agar plate in the absence (Fig. 7a and S4a, ESI†) as well as in the presence of agar-gelatin film (Fig. 7b and S4b, ESI†) without soft nanocomposites. Encouragingly, these nanocomposites (AgNP-**1**–**3**) infused polymeric film exhibited clear zone of inhibition for both Gram-negative, *E. coli* (Fig. 7c–e, respectively) and Gram-positive, *B. subtilis* (Fig. S4c–e, ESI respectively†) bacteria. The measured zone of inhibition (Table S1, ESI†) once again indicates the superior antibacterial activity of AgNP-**1** and AgNP-**2**. However, a zone of inhibition could not be measured in the case of agar-gelatin gel containing AgNP-**4** although the area under AgNP-**4** containing film was free from any bacterial growth (Fig. 7f and S4f, ESI†). Hence, a tissue engineering scaffold has been made to be intrinsically antibacterial by simple infusion of soft nanocomposites.

Now it would be very crucial to see whether the incorporation of AgNP based soft composites (AgNP-**1**–**4**) into this agar-gelatin hybrid has any effect on the biocompatibility of the bactericidal polymeric film. To this end, we investigated the attachment and spreading of NIH3T3 mouse fibroblast cells on agar-gelatin (2 : 1) films with and without AgNP based composites. The cells were seeded in 24 well plates in presence and absence of films in DMEM (Dulbecco's Modified Eagles' Medium) growth media containing 10% FBS (fetal bovine serum). The cell viability was followed after 24 h using LIVE/DEAD® viability/cytotoxicity kit for mammalian cells comprising of calcein-AM (live stain, green fluorescence) and ethidium homodimer (dead stain, red fluorescence).[40] The cells in the control well without any film and well containing agar-gelatin film (in absence of nanocomposites) were found alive as the spindle shaped cells exhibited green fluorescence (Fig. 8a and c)

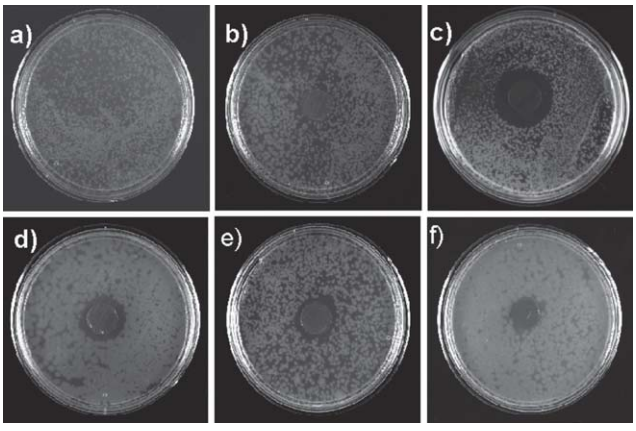

Fig. 7 Antibacterial activity of agar-gelatin films against *E. coli* (a) control without any film (b) agar-gelatin film without AgNP-composites and films containing (c) AgNP-**1**, (d) AgNP-**2**, (e) AgNP-**3** and (f) AgNP-**4** composites.

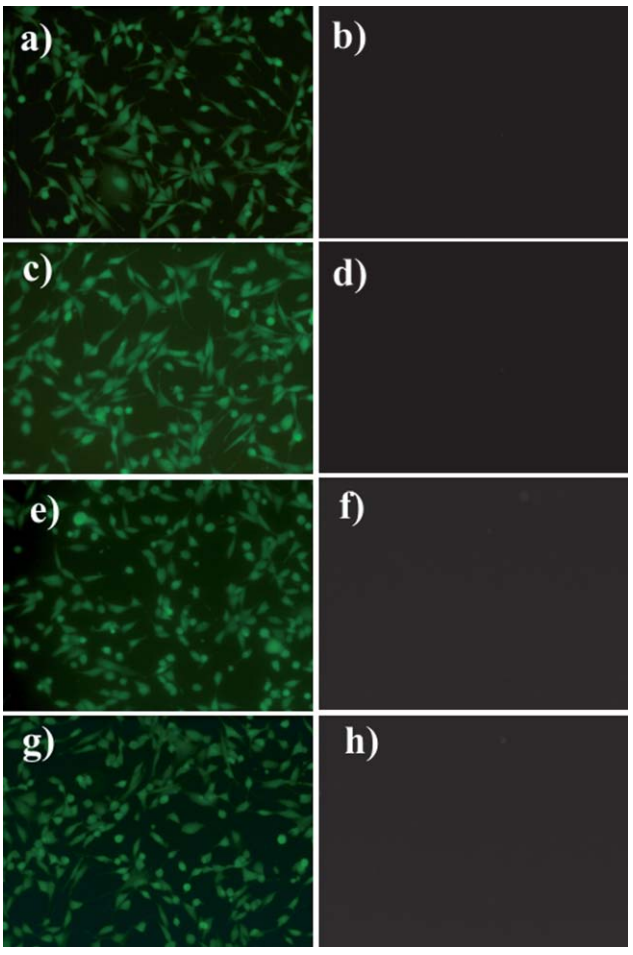

Fig. 8 Fluorescence microscopic images of NIH3T3 cells incubated in control well without any film (a,b); on agar-gelatin film (c,d); on agar-gelatin films containing AgNP-**1**(e,f) and AgNP-**2** (g,h) composites stained with LIVE/DEAD® Viability/Cytotoxicity Kit.

and no red fluorescence (Fig. 8b and d) was observed. Most encouragingly, the NIH3T3 cells adhered on these hydrogels infused with nanocomposites of all the amphiphiles (AgNP-**1** to **4**) showed green luminescence in microscopic images (Fig. 8e,g and S5a,c†) indicating their viability to antibacterial agar-gelatin film. Most of the cells were able to attach and spread on the film as their spindle shape was retained on the surface of the hydrogel film. Also, the absence of any red fluorescence eliminates the possibility of soft nanocomposites induced toxicity to mammalian cells (Fig. 8f,h and S5b,d†). The nanocomposite incorporated agar-gelatin film showed antibacterial activity because of its direct interaction with AgNP possibly through the thiol (–SH) containing protein at the extra cellular membrane of bacteria. Thus, the synthesized AgNP based soft nanocomposites will find immense importance as futuristic antibacterial biomaterial.

Experimental section

Materials

Silica gel of 60–120 mesh, L-tryptophan, L-tyrosine, L-valine, L-isoleucine, *n*-hexadecylamine, *N*,*N*-dicyclohexylcarbodiimide (DCC), 4-*N*,*N*-(dimethylamino) pyridine (DMAP), 1-hydroxybenzotriazole (HOBT), iodomethane, solvents and all other reagents were procured from SRL, India. Water used throughout the study was Milli-Q water. Thin layer chromatography was performed on precoated silica gel 60-F_{254} plates of Merck. $CDCl_3$, uranyl acetate, Amberlite Ira-400 chloride ion exchange resins were obtained from Aldrich Chemical Company. Ethylene diaminetetraacetic acid (EDTA) and reagents required to prepare the nutrient broth culture medium like peptone, yeast extract, and agar powder were purchased from Himedia Chemical Company, India. The LIVE/DEAD® BacLight™ bacterial viability kit, LIVE/DEAD® viability/cytotoxicity kit for mammalian cells were purchased from Molecular Probes, Invitrogen Chemical Company. All the materials used in the cell culture study such as gelatin, DMEM, heat inactivated FBS, trypsin from porcine pancreas and 3-(4,5-dimethyl-2-thiazolyl)-2,5-diphenyl-2*H*-tetrazolium bromide (MTT) were obtained from Sigma Aldrich Chemical Company. ^{1}H NMR spectra were recorded on AVANCE 300MHz (BRUKER) spectrometer. UV-vis spectra were taken in a Cary 50, Varian. Mass Spectrometric (MS) data were acquired by Electron Spray Ionization (ESI) technique on a Q-tof-Micro Quadruple mass spectrophotometer, Micromass.

Synthetic procedure

All amphiphiles (**1–4**, Chart 1) were synthesized and characterized following the previously reported protocol.[23,24] For the synthesis of **1** and **2**, Boc-protected L-amino acids (10 mmol) were coupled with *n*-hexadecylamine (11 mmol) using DCC (11 mmol) and a catalytic amount of DMAP in the presence of HOBT (11 mmol). Boc-protected amide was then purified through column chromatography using 60–120 mesh silica gel and acetone/hexane as the eluent. Deprotections of Boc-groups were carried out using trifluoroacetic acid (TFA, 4 equivalent) in dry DCM (dichloromethane). After 2 h of stirring, solvents were removed on a rotary evaporator and the mixture was taken in ethyl acetate. The ethyl acetate part was thoroughly washed with aqueous 10% sodium carbonate solution followed by brine to neutrality. The organic parts were dried over anhydrous sodium sulphate and concentrated to get the corresponding amines. The produced amines (1 equivalent) were quaternized with excess iodomethane using anhydrous potassium carbonate (2.2 equivalent) and catalytic amount of 18-crown-6-ether in dry DMF for 2 h. The reaction mixtures were taken in ethyl acetate and washed with aqueous sodium thiosulphate and brine solution, respectively. The concentrated ethyl acetate parts were crystallized from methanol/ether to obtain solid quaternized iodides, which were then subjected to ion exchange on an Amberlite Ira-400 chloride ion exchange resin column to get the pure desired amphiphile. Overall yields were in the range of 70–80%. In case of amphiphile **2**, freshly prepared 1 mL of NaOH solution (22 mM) was added to tyrosine containing quaternary ammonium chloride (10 mg, 22 mmol) to make a clear solution. This solution was lyophilized to get the corresponding sodium salt of tyrosine-based amphiphile (**2**).

The dipeptide-based amphiphiles (**3–4**, Chart 1) were also synthesized by the reported protocol. Briefly, methyl ester of an L-amino acid was coupled with C-16 long chain acid chloride in dry chloroform and dry pyridine. The ester protected long chain amide was then purified by column chromatography using 60–120 mesh silica gel and ethyl acetate/hexane as eluent. The product was hydrolyzed using 1 N NaOH (1.1 equivalent) in MeOH for 6 h with stirring at room temperature. Solvents were removed on a rotary evaporator, and the mixture was diluted with water and then washed with ether, followed by acidification by 1 N HCl to get the corresponding carboxylic acid. This acid was then coupled with another methyl ester protected L-amino acid by using DCC, DMAP and HOBt in dry DCM. The purified product was obtained by column chromatography using 60–120 mesh silica gel and ethyl acetate/toluene as eluent. The product was then subjected to hydrolysis by 1 N NaOH (1.1 equivalent) in MeOH for 6 h with stirring at 45–50 °C. The amphiphilic dipeptides with free carboxylic acid end were obtained following the same procedure as described above. Sodium salt of the corresponding carboxylic acid was prepared by dissolving the acid in MeOH and to that 1 equivalent 1 N NaOH (standardized) was added. After brief stirring, the solvent was evaporated and dried to get the sodium salt. The formation of sodium salt was confirmed from FTIR spectroscopy by the disappearance of the –C=O stretching peak of carboxylic acid ~1720–1728 cm^{-1} and also from the improved solubility of the resultant compound in water.

Determination of cmc of the amphiphilic hydrogelators by surface tension measurement

The critical concentration at which the amphiphiles begin to self-assemble was measured from the respective critical micellar concentration (cmc) of the amphiphiles using surface tension method. The cmc of amphiphiles was measured using a tensiometer (Jencon, India) applying the Du Noüy ring method at 25 ± 0.1 °C in water. The cmc values were determined by plotting surface tension (γ) *vs.* concentration of surfactant with the accuracy of ±2% in duplicate experiments.

In situ synthesis of AgNPs

Amphiphiles **1–4** (Chart 1) were used for *in situ* synthesis of AgNPs from Tollens' reagent, which was prepared by drop wise addition of 1 N NaOH solution to 5 mM $AgNO_3$ solution (25 mL) until complete precipitation. The brown precipitate was dissolved in 25% (w/w) ammonia and the clear Tollens' reagent was used for the synthesis of the nanoparticles. To synthesize AgNPs using amphiphile **1**, 5 mg amphiphile was dissolved in 48 mL water in a round bottom flask. The solution was heated to 80 °C and to it 2 mL of 5 mM Tollens' reagent was added. The concentration of both the amphiphile and silver ion (Tollens' reagent) in the total solution was 0.2 mM. The heating was continued and AgNP formation was indicated by the generation of yellow colour in the solution. Time dependent UV-vis spectra were recorded to determine the completion time of the reaction by following the SPR peak of the nanoparticle. In the case of amphiphiles **2**, **3**, and **4** a similar procedure was followed but the concentrations of the amphiphiles and Tollens' reagent were 2 mM and 0.2 mM, respectively. Also, the required temperature for the synthesis of AgNP was 70, 100 and 120 °C, respectively for **2–4**. The solution containing nanoparticles was centrifuged at 30,000 rpm. The pellet was washed thrice by Milli-Q water to remove excess silver ions. The final pellet was dispersed in 5 mL of 0.2 mM amphiphile (addition of this excess surfactant was required for the stabilization of AgNP-composites in nutrient growth media for bacteria) and lyophilized to get nanocomposite powder. This powder (1 mg) was re-dispersed in 500 μL water to get a 2 mg mL^{-1} stock solution, which was used for antibacterial and cell-culture study.

TEM

5 μL of AgNP based composite solution (before centrifugation) was placed on 300-mesh carbon coated copper grid and dried under vacuum for 4 h before taking TEM images with a JEOL JEM 2010 high-resolution microscope. For TEM images of lyophilized nanocomposites (after centrifugation), the dried powder was dissolved in Milli-Q water and then placed on copper grid in similar way as mentioned above. AgNP-**1** and AgNP-**2** composites were negatively stained with uranyl acetate to confirm the presence of self-assemblies of amphiphiles.

XRD

Aqueous solution of AgNP-composites was put on glass slide and dried under vacuum. XRD measurements were done using this slide in a Seifert XRD3000P diffractometer where the source was a Cu-Kα radiation (α = 0.15406 nm) with a voltage and current of 40 kV and 30 mA, respectively.

Quantification of amount of amphiphiles in AgNP based soft composites

Amount of amphiphile in the nanocomposites were measured by UV-vis spectroscopy and TGA. The absorbance value at 280 nm was measured for different amphiphile concentration (**1–4**, Chart 1) to obtain a calibration curve. The amount of amphiphile present in the soft nanocomposite was determined from this calibration curve and thus % of AgNP in nanocomposites was estimated (Table 1). TGA thermograms of representative AgNP-**1** composite and **1** were recorded by using a TA SDT Q600 instrument at a heating rate of 20 °C min^{-1} under a N_2 atmosphere.

Microorganisms and culture conditions

The *in vitro* antimicrobial activity of the amphiphiles and nanocomposites was investigated against both Gram-positive, Gram-negative bacteria. The nutrient broth medium containing peptone (5 g), yeast extract (3 g) in 1 L sterile distilled water at pH 7.0 was used as a liquid medium and nutrient agar [peptone (5 g), yeast extract (3 g) and agar (15 g) in 1 L of sterile distilled water of at pH 7.0] was used as a solid medium in all antibacterial experiments. All the bacteria were purchased from Institute of Microbial Technology, Chandigarh, India. The stock solutions of all the amphiphiles and nanocomposite as well as the required dilutions were made in autoclaved sterile water. For all the bacteria, a representative single colony was picked up with a wire loop and that a loopfull of culture was spread on nutrient agar slant to give single colonies and incubated at 37 °C for 24 h. These fresh overnight cultures of all the bacteria were diluted as required to give a working concentration in the range of 10^6–10^9 colony forming units (cfu)/mL before every experiment.

Antimicrobial studies

MICs of amphiphiles **1–4** as well as the AgNP based soft nanocomposites were estimated by spread plate method. MIC was measured using a series of test tubes containing the amphiphiles (0.05–200 μg mL^{-1}) in 5 mL liquid medium. Diluted microbial culture was added to each test tube in identical concentration to obtain the working concentration of *B. subtilis*, 7.5×10^7–1×10^8 cfu/mL for *S. aureus*; 5×10^6–7.5×10^6 cfu/mL; for *E. coli*, 3.75×10^7–7.5×10^7 cfu/mL; for *K. aerogenes*, 1.5×10^9–6.25×10^9 cfu/mL; for *K. pneumoniae*, 1.4×10^7–7.5×10^7 cfu/mL. All the test tubes were then incubated at 37 °C for 24 h. Then, 50 μL from each tube was spread onto nutrient agar plates inside the laminar hood. Finally, plates were incubated for 24 h at 37 °C and the viable cells were counted. The experiments were performed in triplicate and were repeated twice.

SEM of nanocomposite treated bacteria

E. coli (3.75×10^7 – 7.5×10^7 cfu/mL), *K. aerogenes* (1.5×10^9 – 6.25×10^9 cfu/mL) and *B. subtilis*; (7.5×10^7 – 1×10^8 cfu/mL) *S. aureus* (5×10^6 – 7.5×10^6 cfu/mL) cells (1 mL) were treated with AgNP-**1** composites above MIC at 90 μg mL^{-1} and 25 μg mL^{-1} for Gram-negative and Gram-positive bacteria, respectively. The bacterial cells with and without (untreated cells as control) amphiphile were incubated for 5–6 h. After incubation the mixtures were centrifuged at 5,000 rpm for 5 min. The media was removed completely and the cells were redispersed in 0.9 wt% saline. Finally, 5 μL of the redispersed samples were mounted on a glass slide and dried under vacuum for 4 h and the SEM images were taken on JEOL-6700F scanning electron microscope.

Fluorescence microscopic study for bacteria

The LIVE/DEAD® BacLight™ bacterial kit was used to examine bacterial cell viability under a fluorescence microscope.

The kit contains a mixture of two nucleic-acid binding stains, specifically referred to as SYTO 9 and propidium iodide. The kit was stored at −20 °C in dark, which is taken out and thawed at room temperature just prior to assay. *E. coli* ($3.75 \times 10^7 - 7.5 \times 10^7$ cfu/mL) and *S. aureus* ($5 \times 10^6 - 7.5 \times 10^6$ cfu/mL) cells (1 mL) were treated with AgNP-**1** above MIC (90 μg mL^{-1} for *E. coli* and 25 μg mL^{-1} for *S. aureus*, respectively) and also untreated cells were taken in centrifuge tube as control. The mixtures were centrifuged at 5,000 rpm for 5 min. Then, media was removed completely and the cells were redispersed in 0.9 wt% saline. Finally, BacLight dye mixture (3 μL) was added and incubated in dark at room temperature for 15–20 min. After incubation, 5 μL of the solution mixture was mounted over microscope slides, which was then air-dried and viewed under the microscope (BX61, Olympus) using an excitation filter of BP460-495 nm and a band absorbance filter covering wavelength below 505 nm.

Cell cultures

Mouse fibroblast NIH3T3 cells was obtained from National Center for Cell Science (NCCS), Pune (India), and maintained in DMEM medium supplemented with 10% FBS, 100 mg L^{-1} streptomycin and 100 IU/mL penicillin. Cells were grown in 25 mL cell culture flask and incubated at 37 °C in a humidified atmosphere of 5% CO_2 to approximately 70–80% confluence. Media was changed after every 2–3 days and subculture was performed every 7 days. After 7 days media was removed to eliminate the dead cells. Next, the adherent cells were detached from the surface of the culture flask by trypsinization. Cells were now in the exponential phase of growth for checking the toxicity of the soft nanocomposites.

Cytotoxicity assay

Cytotoxicities of nanocomposites of AgNP-amphiphiles (**1–4**) were assessed by the microculture MTT reduction assay. This assay is based on the reduction of a soluble tetrazolium salt by mitochondrial dehydrogenase of the viable cells to water insoluble coloured product, formazan. The amount of formazan formed can be measured spectrophotometrically after dissolution of the dye in DMSO. The activity of the enzyme and the amount of the formazan produced is proportional to the number of cells alive. Reduction of the absorbance value can be attributed to the killing of the cells or inhibition of cell proliferation by the composites. Cells were seeded at a density of 15,000 cells per well in a 96-well microtiter plate for 18–24 h before the assay. Stock solutions of all the composites were prepared in water. Sequential dilutions of these stock solutions were done during the experiment to vary the concentrations (10 to 200 μg mL^{-1}) in the microtiter plate. The cells were incubated for 4 h at 37 °C under 5% CO_2. Then, 15 μL MTT stock solution (5 mg mL^{-1}) in phosphate buffer saline was added to the above mixture and the cells were further incubated for 4 h. The precipitated formazan was dissolved thoroughly in DMSO and absorbance at 570 nm was measured using BioTek® Elisa Reader. The number of surviving cells were expressed as percent viability = (A_{570}(treated cells) − background/A_{570}(untreated cells) − background) × 100.

Preparation of agar-gelatin gel film

The mixture (1 wt%) of agar and gelatin at ratio of 2 : 1 taken in PBS (pH 7.4) was dissolved by heating the solution. In case of AgNP containing film preparation, nanocomposite solution was added to this homogeneous mixture of agar and gelatin so that 50 μg mL^{-1} of AgNP-**1/2** and 200 μg mL^{-1} of AgNP-**3/4** could be attained. Then, glutaraldehyde (0.15 wt%) was added to the hot solution for cross linking of the components in the solution. Each solution (1 mL) was poured into 24-wells tissue culture flask and was allowed to form gel at room temperature for overnight. Then plates containing gels were dried in an incubator for 12 h at 50 °C to form thin films. These prepared films were treated with 0.1 mM glycine for 1 h to block the remaining aldehyde group. The films were then washed several times with Milli-Q water to remove excess glycine and then with PBS to neutralize the surface. These films were then again dried and UV sterilized overnight and kept in sterile vacuum desiccators for further experiment.

Antibacterial activity of agar-gelatin films

The antibacterial activity of agar-gelatin films against *E. coli* and *B. Subtilis* was followed in nutrient agar plates. For this, each bacterium was cultured on nutrient agar slant at 37 °C for 24 h. These overnight cultures of bacteria were diluted as required to get a concentration ~10^5 cfu/mL. This bacteria containing solution (1 mL) was added to nutrient agar plate. After the agar plate became dry in 30 min, the agar-gelatin films with and without AgNP was placed on the middle of the agar plates. The plates were then incubated for 24 h at 37 °C. The bacteria killing ability of the films was followed by measuring the zone of inhibition in the agar plate.

Biocompatibility of agar-gelatin films

The NIH3T3 cell attachment studies were done on control well (24 well plate) without any film and on agar-gelatin films with and without AgNP based composites. Films were incubated with DMEM media (1 mL) containing 10% FBS. After 3 h the media was removed and 5×10^5 cells were seeded in each well with 1 mL media. The cells were incubated for 24 h in a 5% CO_2 atmosphere. After 24 h the adherent cells were washed with PBS and cell viability was examined under a fluorescence microscope using the LIVE/DEAD® viability/cytotoxicity kit for mammalian cells. The kit contains a mixture of two nucleic acid binding stains, specifically referred to as Calcein AM and Ethidium homodimer-1 (EthD-1). The kit was stored at −20 °C in dark, and was taken out and thawed at room temperature just prior to assay. The supplied 2 mM EthD-1 stock solution (4 μL) was added to 2 mL of sterile, tissue culture-grade PBS and the mixture was vortexed to ensure thorough mixing. The supplied 4 mM calcein AM stock solution (1 μL) was then added to the 2 mL EthD-1 solution and vortexed. The final stock solution (500 μL) of calcein AM (2 μM) and EthD-1 (4 μM) was then added directly to each well containing NIH3T3 cells. After 30 min incubation with the fluorescent dye, the cells were viewed under Olympus IX51 inverted microscope (ex/em ~495 nm/515 nm for calcein AM and ex/em ~ 495 nm/635 nm) for EthD-1.

Conclusion

In summary, the newly developed AgNP based soft nanocomposites by *in situ* synthesis of AgNPs within the self-assemblies of amphiphilic hydrogelators have potent antibacterial activity against both Gram-positive and Gram-negative bacteria. Importantly, the intrinsic Gram-positive bacteria killing efficacy of the cationic amphiphiles was complemented in the presence of AgNPs, as the nanocomposite were lethal towards both types of bacteria. Furthermore, the structure of the amphiphile was also altered in order to understand the specific roles of the charge and nature of the head group on the synthesis and stabilization of AgNPs as well as in modulating the bactericidal efficacy. Encouragingly, when these AgNP-composites were incorporated into well know tissue engineering scaffold agar-gelatin films, they were able to kill both Gram-positive and Gram-negative bacteria despite being non-toxic toward mammalian cells. Therefore, the designed soft nanocomposite promises to have immense implications in biomedicine including tissue engineering.

Acknowledgements

P.K.D. is thankful to Department of Science and Technology, India for financial assistance. A.S., S.D. and S.M. acknowledge Council of Scientific and Industrial Research, India for Research Fellowships.

References

1 A. Makovitzki, D. Avrahami and Y. Shai, *Proc. Natl. Acad. Sci. U. S. A.*, 2006, **103**, 15997.
2 A. Rai, A. Prabhuneb and C. C. Perry, *J. Mater. Chem.*, 2010, **20**, 6789; S. Pritz, M. Pätzel, G. Szeimies, M. Dathea and M. Bienert, *Org. Biomol. Chem.*, 2007, **5**, 1789; A. Zumbuhel, L. Ferreira, D. Kuhn, A. Astashkina, L. Long, Y. Yeo, T. Iaconis, M. Ghannoum, G. R. Fink, R. Langer and D. S. Kohane, *Proc. Natl. Acad. Sci. U. S. A.*, 2007, **104**, 12994; B. Xing, C.-W. Yu, K.-H. Chow, P.-L. Ho, D. Fu and B. Xu, *J. Am. Chem. Soc.*, 2002, **124**, 14846; Z. Yang, K. Xu, Z. Guo, Z. Guo and B. Xu, *Adv. Mater.*, 2007, **19**, 3152; J. C. Tiller, *Angew. Chem., Int. Ed.*, 2003, **42**, 3072; J. C. Tiller, S. B. Lee, K. Lewis and A. M. Klibanov, *Biotechnol. Bioeng.*, 2002, **79**, 465.
3 S. A. Sieber and M. A. Marahiel, *Chem. Rev.*, 2005, **105**, 715; E. D. Brown and G. D. Wright, *Chem. Rev.*, 2005, **105**, 759; J. Haldar, P. Kondaiah and S. Bhattacharya, *J. Med. Chem.*, 2005, **48**, 3823; C. J. Waschinski, J. Zimmermann, U. Salz, R. Hutzler, G. Sadowski and J. C. Tiller, *Adv. Mater.*, 2008, **20**, 104; C. J. Waschinski, S. Barnert, A. Theobald, R. Schubert, F. Kleinschmidt, A. Hoffmann, K. Saalwächter and J. C. Tiller, *Biomacromolecules*, 2008, **9**, 1764.
4 A. Panáček, L. Kvítek, R. Prucek, M. Kolář, R. Večeřová, N. Pizúrová, V. K. Sharma, T. Nevěčná and R. Zbořil, *J. Phys. Chem. B*, 2006, **110**, 16248; J. R. Morones, J. L. Elechiguerra, A. Camacho, K. Holt, J. B. Kouri, J. T. Ramírez and M. J. Yacaman, *Nanotechnology*, 2005, **16**, 2346; M. Rai, A. Yadav and A. Gade, *Biotechnol. Adv.*, 2009, **27**, 76; J. Jain, S. Arora, J. M. Rajwade, P. Omray, S. Khandelwal and K. M. Paknikar, *Mol. Pharmaceutics*, 2009, **6**, 1388.
5 N. S. Wigginton, A. D. Titta, F. Piccapietra, J. Dobias, V. J. Nesatyy, M. J. F. Suter and R. Bernier-Latmani, *Environ. Sci. Technol.*, 2010, **44**, 2163.
6 H. H. Lara, N. V. Ayala-Núñez, L. d. C. I. Turrent and C. R. Padilla, *World J. Microbiol. Biotechnol.*, 2010, **26**, 615.
7 L. Kvítek, A. Panáček, J. Soukupová, M. Kolář, R. Večeřová, R. Prucek, M. Holecová and R. Zbořil, *J. Phys. Chem. C*, 2008, **112**, 5825.
8 J. S. Kim, E. Kuk, K. N. Yu, J.-H. Kim, S. J. Park, H. J. Lee, S. H. Kim, Y. K. Park, Y. H. Park, C.-Y. Hwang, Y.-K. Kim, Y.-S. Lee, D. H. Jeong and M.-H. Cho, *Nanomed.: Nanotechnol., Biol. Med.*, 2007, **3**, 95.
9 X. Xu and M. Zhou, *Fibers Polym.*, 2008, **9**, 685.
10 Y.-C. Chung, I.-H. Chen and C.-J. Chen, *Biomaterials*, 2008, **29**, 1807.
11 A. Travan, C. Pelillo, I. Donati, E. Marsich, M. Benincasa, T. Scarpa, S. Semeraro, G. Turco, R. Gennaro and S. Paoletti, *Biomacromolecules*, 2009, **10**, 1429.
12 V. K. Sharma, R. A. Yngard and Y. Lin, *Adv. Colloid Interface Sci.*, 2009, **145**, 83; A.-T. Le, P. T. Huy, P. D. Tam, T. Q. Huy, P. D. Camb, A. A. Kudrinskiy and Y. A. Krutyakov, *Curr. Appl. Phys.*, 2010, **10**, 910.
13 S. Roy and P. K. Das, *Biotechnol. Bioeng.*, 2008, **100**, 756.
14 R. N. Mitra, A. Shome, P. Paul and P. K. Das, *Org. Biomol. Chem.*, 2009, **7**, 94.
15 J. W. Costerton and K. J. Cheng, *J. Antimicrob. Chemother.*, 1975, **1**, 363.
16 S. P. Denyer and J. Y. Maillard, *J. Appl. Microbiol.*, 2002, **92**, 35S.
17 V. Verma, P. Verma, S. Kar, P. Ray and A. R. Ray, *Biotechnol. Bioeng.*, 2007, **96**, 392.
18 M. Uygun, M. U. Kahveci, D. Odaci, S. Timur and Y. Yagci, *Macromol. Chem. Phys.*, 2009, **210**, 1867; Y.-Q. Ma, J.-Z. Yi and L.-M. Zhang, *J. Macromol. Sci., Part A: Pure Appl. Chem.*, 2009, **46**, 643; H. Basit, A. Pal, S. Sen and S. Bhattacharya, *Chem.–Eur. J.*, 2008, **14**, 6534; A. Pal, H. Basit, S. Sen, V. K. Aswal and S. Bhattacharya, *J. Mater. Chem.*, 2009, **19**, 4325; A. Pal, A. Srivastava and S. Bhattacharya, *Chem.–Eur. J.*, 2009, **15**, 9169.
19 P. R. Selvakannan, S. Mandal, S. Phadtare, A. Gole, R. Pasricha, S. D. Adyanthaya and M. Sastry, *J. Colloid Interface Sci.*, 2004, **269**, 97.
20 S. K. Bhargava, J. M. Booth, S. Agrawal, P. Coloe and G. Kar, *Langmuir*, 2005, **21**, 5949.
21 S. Si and T. K. Mandal, *Chem.–Eur. J.*, 2007, **13**, 3160; R. N. Mitra and P. K. Das, *J. Phys. Chem. C*, 2008, **112**, 8159; T. Kar, S. Dutta and P. K. Das, *Soft Matter*, 2010, **6**, 4777.
22 S. Si, E. Dinda and T. K. Mandal, *Chem.–Eur. J.*, 2007, **13**, 9850; S. Si, R. R. Bhattacharjee, A. Banerjee and T. K. Mandal, *Chem.–Eur. J.*, 2006, **12**, 1256.
23 T. Kar, S. Debnath, D. Das, A. Shome and P. K. Das, *Langmuir*, 2009, **25**, 8639; A. Shome, S. Debnath and P. K. Das, *Langmuir*, 2008, **24**, 4280.
24 D. Das, A. Dasgupta, S. Roy, R. N. Mitra, S. Debnath and P. K. Das, *Chem.–Eur. J.*, 2006, **12**, 5068; S. Roy, A. Dasgupta and P. K. Das, *Langmuir*, 2007, **23**, 11769; D. Das, S. Roy, S. Debnath and P. K. Das, *Chem. Eur. J.*, 2010, **16**, 4911; S. Dutta, A. Shome, S. Debnath and P. K. Das, *Soft Matter*, 2009, **5**, 1607.
25 S. Roy, D. Das, A. Dasgupta, R. N. Mitra and P. K. Das, *Langmuir*, 2005, **21**, 10398; A. Shome, T. Kar and P. K. Das, *ChemPhysChem*, 2011, **12**, 369, DOI: 10.1002/cphc.201000708.
26 C. H. B. Ng, J. Yang and W. Y. Fan, *J. Phys. Chem. C*, 2008, **112**, 4141.
27 V. Sambhy, M. M. MacBride, B. R. Peterson and A. Sen, *J. Am. Chem. Soc.*, 2006, **128**, 9798.
28 W. W. Wilsona, M. M. Wadeb, S. C. Holmana and F. R. Champlin, *J. Microbiol. Methods*, 2001, **43**, 153.
29 R. Kügler, O. Bouloussa and F. Rondelez, *Microbiology*, 2005, **151**, 1341.
30 J. A. Castillo, P. Clapes, M. R. Infante, J. Comas and A. Manresa, *J. Antimicrob. Chemother.*, 2006, **57**, 691.
31 C. J. Ioannou, G. W. Hanlon and S. P. Denyer, *Antimicrob. Agents Chemother.*, 2007, **51**, 296.
32 E. Jawetz, J. L. Melnick, E. A. Adelberg, G. F. Brooks, J. S. Butel and L. N. Ornston, *Medical microbiology*, Prentice-Hall, London, 1989, pp. 46.
33 T. J. Franklin and G. A. Snow, *Antiseptics, Antibiotics, and the Cell Membrane, Biochemistry of Antimicrobial Action*, Chapman and Hall Ltd., London, 1981, pp. 58.
34 K. K. Y. Wong and X. Liu, *Med. Chem. Commun.*, 2010, **1**, 125.
35 M. L. Mangoni, N. Papo, D. Barra, M. Simmaco, A. Bozzi, A. Di Giulio and A. C. Rinaldi, *Biochem. J.*, 2004, **380**, 859.
36 S. Sharma, P. Sen, S. N. Mukhopadhyay and S. K. Guha, *Colloids Surf., B*, 2003, **32**, 43.
37 L. Boulos, M. Prevost, B. Barbeau, J. Coallier and R. Desjardins, *J. Microbiol. Methods*, 1999, **37**, 77.

38 S. Munro, *Cell*, 2003, **115**, 377; F. J. Alvarez, L. M. Douglas and J. B. Konopka, *Eukaryotic Cell*, 2007, **6**, 755.
39 V. Jayawarna, M. Ali, T. A. Jowitt, A. F. Miller, A. Saiani, J. E. Gough and R. V. Ulijn, *Adv. Mater.*, 2006, **18**, 611; S. J. Todd, D. Farrar, J. E. Gough and R. V. Ulijn, *Soft Matter*, 2007, **3**, 547; M. Zhou, A. M. Smith, A. K. Das, N. W. Hodson, R. F. Collins, R. V. Ulijn and J. E. Gough, *Biomaterials*, 2009, **30**, 2523; R. V. Ulijn and D. N. Woolfson, *Chem. Soc. Rev.*, 2010, **39**, 3349.
40 K. Vasilev, V. Sah, K. Anselme, C. Ndi, M. Mateescu, B. Dollmann, P. Martinek, H. Ys, L. Ploux and H. J. Griesser, *Nano Lett.*, 2010, **10**, 202; V. Jayawarna, A. Smith, J. E. Gough and R. V. Ulijn, *Biochem. Soc. Trans.*, 2007, **35**, 535.

